ICSV14
Cairns • Australia
9-12 July, 2007

14th International Congress on Sound & Vibration

ACOUSTIC HOLOGRAPHY BASED ON THE INVERSE-BEM FOR THE SOURCE IDENTIFICATION OF MACHINERY NOISE

Jeong-Guon Ih

Centre for Noise and Vibration Control (NoViC), Department of Mechanical Engineering
Korea Advanced Institute of Science and Technology (KAIST)
Science Town, Daejeon 305-701, Korea
J.G.Ih@kaist.ac.kr

Abstract

Near-field acoustical holography (NAH) is an indirect method for the identification of vibro-acoustic properties of vibrating sound sources. In this technique, acoustic properties on the source plane can be inversely reconstructed, using the field pressure, which is measured on the measurement or hologram plane. The sound radiation, diffraction and transmission between the vibrating source and the measurement field can be modelled by the vibro-acoustic transfer matrix using the boundary element method (BEM). Consequently, the distribution of the surface velocities of the arbitrary shaped source, not on the near-field 'source' plane, can be reconstructed by multiplying the inverse of the calculated vibro-acoustic transfer matrix and the measured field pressure vector at any shape of near-field plane, including the conformal one. This type of conformal NAH technique has the following advantages compared with conventional NAH based on the spatial Fourier transform. One can deal with the complex shaped sources that cannot be described by separable coordinates; the pressure need not be measured in separable coordinates, thus a reduced number of measurements with uneven spacing is possible; reflections from all directions can be considered; concave regions of the source can be reconstructed; and wrap-around error due to the finite aperture size is not involved. In this paper, the basic nature of the involved problems is explained and a procedure for realizing the inverse identification of the machine noise source is demonstrated in several practical applications.

1. INTRODUCTION

Information on surface velocity, pressure, intensity, acoustic power, and field intensity vector of the vibro-acoustic system is very useful in the early stage of effective noise control, either by passive or active means. Therefore, one can regard the identification of source distribution as the starting point for the effective noise control, although difficulties exist in dealing with the extended vibro-acoustic radiators. The actual extended sound radiators are continuous in geometry, irregular in shape with some inaccessibly small spaces sometimes, wide in radiated sound spectra, complicated in modal behaviour and severe interactions, harsh in operating conditions like temperature and toxic gases, and usually located in a noisy environment during operation. Such hard conditions of practical vibro-acoustic sources cause tremendous difficulties in source identification by the direct measurement techniques using sensors like accelerometer, strain gage, LDV, gap sensor, potentiometer, etc. Consequently, one needs the inverse or indirect techniques [1-4] for solving various acoustic problems including the vibro-acoustic radiation case.

For the vibro-acoustic source identification, many theoretical and experimental techniques have been developed either using direct method or indirect one: selective operation, cocooning, window method, duct connection, nearfield pressure or motion measurement, direct measurement of surface vibration, directional microphones, sound intensimetry, surface intensity technique, beamforming, optical and acoustical holography, vectorial analysis or transfer path analysis, signal processing techniques, and so forth. Among these direct and indirect techniques, the most popular indirect method has been the sound intensimetry. However, it should be reminded that the source activity identified by sound intensimetry is not an actual source property, but a field data. Furthermore, the excessive reactivity in the measurement field will cause a severe problem in detecting the real source. Another popular and seemingly precise technique for the source identification is the laser holography. Use of scanning laser holography (SLDV) and dual-pulsed laser Doppler interferometry are facilitated in a very controlled environment and steady state source operation condition; whereas the electronic speckle pattern interferometry can be used in 2-D painted source field, but, at the moment, it is implemented with a high cost.

Nearfield acoustical holography (NAH) is an indirect method using the array microphones for the inverse identification of vibro-acoustic properties of sound sources. In this technique, the acoustic properties on the source plane can be reconstructed, using the field pressure, which is measured on the measurement or hologram plane. Of the two major techniques that have been a great stimulus to the development of NAH, one is based on the spatial Fourier transform and the other on the acoustic boundary element method (BEM). In the former method, the field pressures, which are measured on a hologram plane, are decomposed into space and wave number domains by spatial Fourier transform. The pressure decay in propagation can be compensated and the pressure on a target plane is then reconstructed by an inverse spatial Fourier transform [5-7]. This technique was commercially implemented earlier [8]. The shape of the source surface should be regular, and, if this is not the case, then a hypothetical regular plane near the actual source surface needs to be assumed for the reconstruction. In the latter approach, the geometric and vibro-acoustic relation between the sound source and the hologram or measurement plane is modelled as the vibro-acoustic transfer matrix by numerically implementing the integral equations for acoustics [9-11]. The sound radiation and transmission between the vibrating source and the measurement field (or hologram plane) can be modelled by the vibro-acoustic transfer matrix by using boundary integral equation or its discretized form of the BEM. Consequently, the distribution of the surface velocities of the source can be reconstructed by multiplying the inverse of the calculated vibro-acoustic transfer matrix and the measured field pressure vector at any shape of near-field plane, including the conformal one. This type of conformal NAH is capable of dealing with the complex shaped sources that cannot be described by separable coordinates.

The other technique worth mentioning is the method using a series expansion of spherical radiation functions for describing the sound field, in particular, in the hologram plane. The coefficient of each spherical function, centrally located at an origin within the source volume, is determined by the numerical inverse process [12,13]. In a similar concept, the equivalent source method (ESM) [14] that can be also used for the reconstruction of sound field [15,16]. The Helmholtz equation least-squares method [17], which is a special case of ESM by using spherical waves, emanating from a single point, has been suggested for reconstructing the sound field or source field in the spherical coordinates. It was shown [16,18] that this method can be combined with the BEM-based NAH method, with relatively fewer measurements, for the reconstruction of source parameters of an arbitrarily shaped object. The main topic of this paper will be confined only to the BEM-based NAH (or NAH based on the inverse BEM). Another indirect identification technique with great potential in practice is the inverse frequency response function (FRF) method [19]. This method is based on the transfer path information between inputs on a surface and outputs measured on the microphones. Once the pseudo-inverse of FRF is determined by using, in general, over-determined least-squared solution approach and singular value decomposition, the unknown inputs of the system (usually the volume velocity of a source segment) can be identified from the measured pressure. Application to an automobile interior to optimize the sound insulation material was reported [20]. An overview of the inverse reconstruction problem by using the acoustical holography can be found in Ref [21].

The basic concept of the BEM-based NAH was first explicitly studied by Gardner and Bernhard [9], who introduced the source identification method in the highly reactive field by utilizing direct BEM. Veronesi and Maynard [10] utilized the singular value decomposition of the discretized direct boundary integral equation, in order to decompose the field and source properties into the wave-vector domain. They demonstrated that the suppression of the amplification effect of the measurement noise via the rejection of higher wave-vector mode components led to an improved resolution. Bai [22] formulated the generalized holography equation based on direct BEM. He represented all possible combinations of the transfer matrix, in order to correlate the particle velocity and field pressure on the source surface and the field plane. Kim and Ih [23] described a resolution enhancement technique using the optimal selection of measurement points and regularization of the transfer matrix for the interior problem. By utilizing a trade-off relationship between variance and bias errors, the optimal rank, which produces the minimum mean square error could be determined. Zhang, et al. [24] employed the indirect formulation for the BEM-based NAH. Valdivia and Williams [25] suggested the iterative technique, which can avoid using the singular value decomposition technique that may be beneficial in dealing with a large transfer matrix.

As aforementioned, the BEM-based NAH technique thus provides a good opportunity for restoring the vibro-acoustic field of many practical arbitrarily shaped sources. Its optimal feature is that only the measured field pressure is required for determining pressure, particle velocity, surface admittance, intensity, and power flow of the source and the domain of interest as well. This type of conformal NAH technique has the following advantages compared with conventional NAH based on the spatial Fourier transform. One can deal with the complex shaped sources that cannot be described by separable coordinates; the pressure need not be measured in separable coordinates, thus a reduced number of measurements with uneven spacing is possible; reflections from all directions can be considered; concave regions of the source can be reconstructed; and wrap-around error due to the finite aperture size is not involved. However, this method has some inconvenient aspects as well. The acoustic and geometric relation of the source surface and the hologram plane should be modelled via the use of the BEM and this causes problems. A considerable number of boundary elements and nodes are ultimately required for modelling the actual source surfaces involved in a practical noise problem and the amount of field pressure data increases in parallel with that of the surface nodes. The applicable frequency range can be limited by the characteristic length of the typical element. In addition, care should be taken with respect to the inversion of the fully populated vibro-acoustic transfer matrix that has a high singularity. However, if such difficulties are somehow overcome with some technical labour, the drawback of additional BEM modelling may not be a big loss after all because one needs the BEM model of the irregular ‘source’ for the eventual forward prediction of the sound field, anyway. In this paper, the basic nature of the involved problems is explained and a procedure for realizing the inverse identification of the machine noise source is demonstrated in several practical applications.

2. SUMMARY OF THEORETICAL BACKGROUND

2.1 Sound Radiation from an Extended Source and Its Boundary Element Modelling

Assume that the domain, $\boldsymbol{V}$, enclosed by the boundary, $\boldsymbol{S}_o$, is filled with an isothermal, homogeneous, inviscid, compressible, and stationary fluid medium, which is disturbed by a time harmonic ($\sim e^{j\omega t}$) acoustic field. The acoustic pressure p at a position $\boldsymbol{r}$ produced by the harmonic vibration of the surface S and the distributed internal source f in a volume V is given by the following Kirchhoff-Helmholtz integral equation:

$$c(\boldsymbol{r})p(\boldsymbol{r}) = -\int_{S_o}\left[p(\boldsymbol{r}_o)\left(\frac{1}{R}+ik\right)\frac{\exp(-ikR)}{R}\cos\theta + i\omega\rho v(\boldsymbol{r}_o)\frac{\exp(-ikR)}{R}\right]dS + \int_V f(\boldsymbol{r}_0)G(\boldsymbol{r},\boldsymbol{r}_0)dV \quad . \tag{1}$$

Here, k is the wave number, $\boldsymbol{r}_0$ the position vector of a surface point, R the distance between two points, G the Green function, ρ the density of the fluid medium, and v the surface velocity. The first integrand of Eq.(1) has the directivity of $\cos\theta$ and means the dipole effect by the surface pressure $p(\boldsymbol{r}_o)$. The second integrand shows the monopole effect by the surface normal velocity $v(\boldsymbol{r}_o)$. The last term is the distributed internal source effect in the domain of interest.

If discrete field points and surface points are considered, due to practical reason, and $\boldsymbol{p}_s$, $\boldsymbol{v}_s$ denote pressure and normal velocity vectors on the surface nodes, respectively, the forgoing K-H integral equation can be approximated by the matrix equation form as

$$[D]_s\{p\}_s = [M]_s\{v\}_s \quad \text{on the boundary,} \tag{2}$$

$$\{p\}_f = [D]_f\{p\}_s + [M]_f\{v\}_s \quad \text{in the domain.} \tag{3}$$

Here, $[D]_s$ and $[M]_s$ indicate the dipole (including the solid angle information) and monopole matrices on the surface, and $[D]_f$ and $[M]_f$ are those corresponding to field pressures, respectively. If the Neumann, Dirichlet, and Robin boundary conditions coexist, from the given boundary conditions, $\{\boldsymbol{p}_1, \boldsymbol{v}_2\}_s$ and z_3, Eq. (2) can be rewritten to calculate $\{\boldsymbol{v}_1, \boldsymbol{p}_2, \boldsymbol{p}_3\}_s$ as

$$\begin{bmatrix} -\boldsymbol{M}_{11} & \boldsymbol{D}_{12} & \boldsymbol{D}_{13}-\boldsymbol{M}_{13}/z_3 \\ -\boldsymbol{M}_{21} & \boldsymbol{D}_{22} & \boldsymbol{D}_{23}-\boldsymbol{M}_{23}/z_3 \\ -\boldsymbol{M}_{31} & \boldsymbol{D}_{32} & \boldsymbol{D}_{33}-\boldsymbol{M}_{33}/z_3 \end{bmatrix}_s \begin{Bmatrix} \boldsymbol{v}_1 \\ \boldsymbol{p}_2 \\ \boldsymbol{p}_3 \end{Bmatrix}_s = \begin{bmatrix} -\boldsymbol{D}_{11} & \boldsymbol{M}_{12} \\ -\boldsymbol{D}_{21} & \boldsymbol{M}_{22} \\ -\boldsymbol{D}_{31} & \boldsymbol{M}_{32} \end{bmatrix}_s \begin{Bmatrix} \boldsymbol{p}_1 \\ \boldsymbol{v}_2 \end{Bmatrix}_s , \tag{4}$$

where z_3 represents the acoustic impedance. If the Neumann boundary conditions are considered only, on the condition that $[D]_s^{-1}$ exists, the field pressure can be expressed as

$$\{p\}_f = ([M]_f + [D]_f[D]_s^{-1}[M]_s)\{v\}_s \equiv [G]\{v\}_s , \tag{5}$$

where $[G]$ is the vibro-acoustic transfer matrix that correlates the surface normal velocity with the field pressure and contains geometric information concerning the system as well.

2.2 Inverse Operation and Relevant Physical Meanings

Equation (5) should be inverted to obtain the source data; however, [G] is in general non-square and complex. If the field pressure is known at m points, the surface velocity at n (preferably smaller than m for a good result) nodes can be uniquely determined by utilizing a least-squared solutions approach and singular value decomposition (SVD). The SVD of $[G]$ provides the acoustical modal expansion between the hologram and source field [26]. The transfer matrix [G] can be decomposed by

$$[G]=[U][\Lambda][W]^H , \tag{6}$$

where

$$[\Lambda]=diag(\lambda_1,\lambda_2,..... ,\lambda_n), \ \lambda_1 \ge \lambda_2 \ge ..... \ge \lambda_n \ge 0, \ \{u_i\}^H\{u_j\} = \delta_{ij}, \quad \{w_i\}^H\{w_j\} = \delta_{ij} . \tag{7}$$

Here, δ_{ij} is the Kronecker delta, the superscript "H" signifies the Hermitian operator, and the subscript "n" is the rank of **[*G*],** the elements of diagonal matrix $[\Lambda]$ are singular values λ_i, and $[U]$, $[W]$ indicate the left and right singular vectors, each of which has orthonormal columns. By virtue of the SVD, the inverse of Eq. (5) can be expressed as

$$\{v\}_s = [G]^+\{p\}_f = ([G]^H[G])^{-1}[G]^H\{p\}_f \ = [W][\Lambda]^{-1}[U]^H\{p\}_f \ . \tag{8}$$

Here, $[G]^+$ denotes the n x m pseudoinverse matrix. Equation (8) enables the reconstruction of the velocity field on the source surface, in principle, if the field pressures are measured and the transfer matrix is generated by the BEM. Figure 1 shows a parallelepiped radiator model and Fig. 2 is the given (true) velocity of the vibrating plate on the top. Figures 3-5 illustrate typical shapes of w_i, λ_i, and u_i, respectively.

Physically, $\{u_i\}$ and $\{w_i\}$ indicate the wave-vectors which decompose the distribution of field pressure and surface velocity on the hologram and source planes for a selected frequency. Mutually orthogonal wave-vectors constitute the eigenspace of the measurement and source fields. The physical meaning of λ_i is the weighting factor for converting these field vectors from the source surface into the hologram plane. Conversely, each singular value represents the

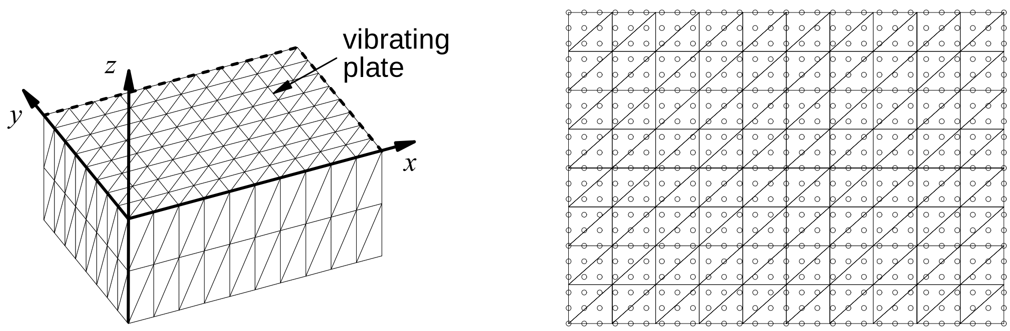

Fig.1. (a) Boundary element model of a parallelepiped box ($700^L \times 520^W \times 320^H$ mm, 234 nodes, 63 velocity-unknown nodes, 464 linear elements), (b) 609 field points for the measurement.

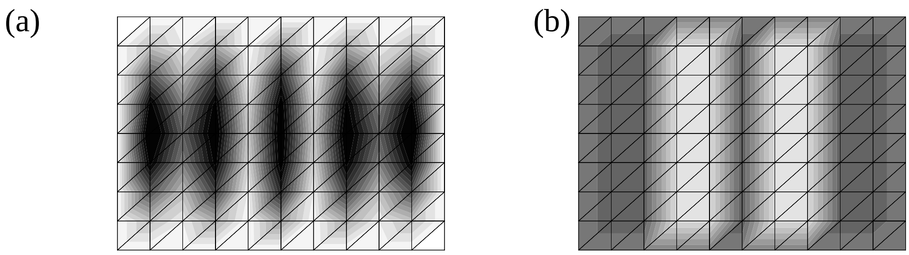

Fig.2. Source velocity on the top of a box for (5,1) mode (163 Hz). (a) amplitude, (b) phase.

contribution of an acoustic mode on the source field to that of the measurement field [27]. High order modes corresponding to the components with small singular values are non-propagating wave components that decay out fast in the nearfield.

2.3 Ill-conditioned Nature and Regularization for Image Enhancement

Generally, the source reconstruction problem involves the inverse process of an ill-conditioned matrix. This rank deficiency is due to small singular values that result in the condition number being much larger than unity. The main cause is the error generated from the measurement noise that is inevitably included in the observed field pressure and the numerical noise, which

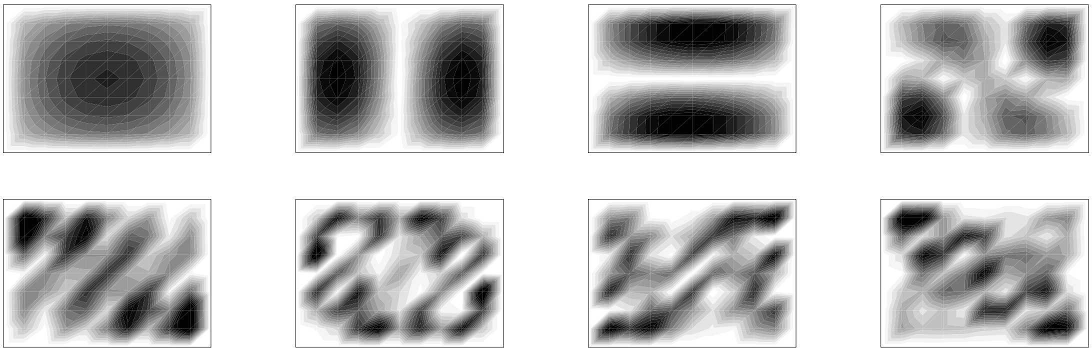

Fig.3. Magnitude shapes of right singular vectors: (a) $\{w_1\}$, (b) $\{w_2\}$, (c) $\{w_3\}$, (d) $\{w_4\}$, (e) $\{w_{10}\}$, (f) $\{w_{20}\}$, (g) $\{w_{30}\}$, (h) $\{w_{40}\}$.

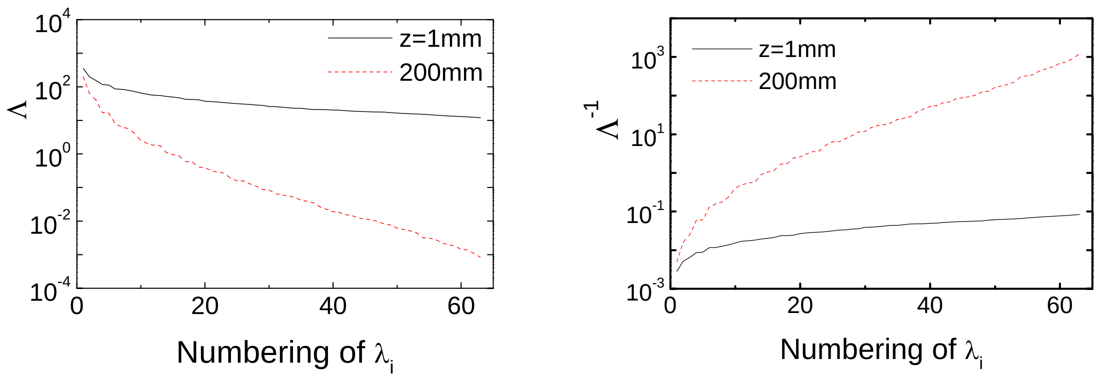

Fig. 4. Magnitudes of singular values of the transfer matrix. z is the distance of the hologram plane.

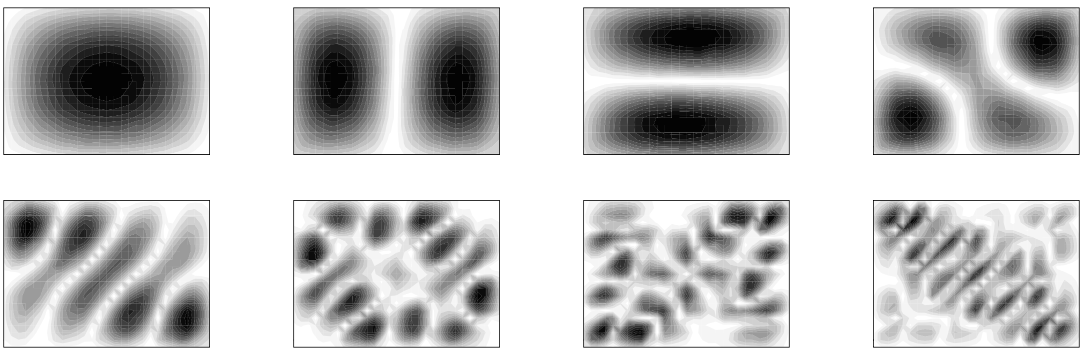

Fig. 5. Magnitude shapes of left singular vectors: (a) $\{u_1\}$, (b) $\{u_2\}$, (c) $\{u_3\}$, (d) $\{u_4\}$, (e) $\{u_{10}\}$, (f) $\{u_{20}\}$, (g) $\{u_{30}\}$, (h) $\{u_{40}\}$.

occurs in the computation. In the inverse calculation, the high-order small singular values will amplify the non-propagating wave components. The contaminating noise in the measured field pressure will also be amplified during this process and this will yield highly distorted reconstructed data. Figure 6 depicts noise contaminated (S/N ratio=30) field pressure data at two hologram planes. Figures 4(b) and 7 show the inverse of [Λ] and its effect to the inversely projected vectors. One can find the blurred reconstruction image of the source in Fig. 8.

To overcome the divergence phenomenon due to non-propagating wave components, proper filtering is needed during the inverse operation [23]. Because the higher-order modes in acoustical holography can be considered as non-propagating wave components, low-pass filtering such as the Wiener filtering [28,29] can be taken in the optimal sense, and spatial regularization by using the singular value decomposition (SVD) is adopted [23,30] for taking account of the measurement noise. Another possible approach is regularization by using an iterative inverse solution [31,32]. This method in the image restoration area has been known that it does not require an inverse matrix and the precision of solutions can be enhanced by

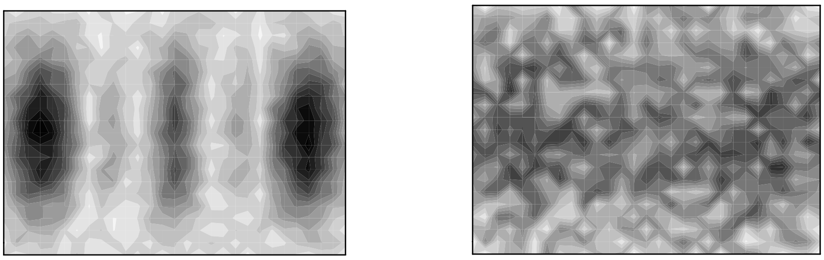

Fig. 6. Amplitude of given (estimated) field pressure with measurement noise (S/N ratio = 30): (a) z=1 mm, (b) z=200 mm.

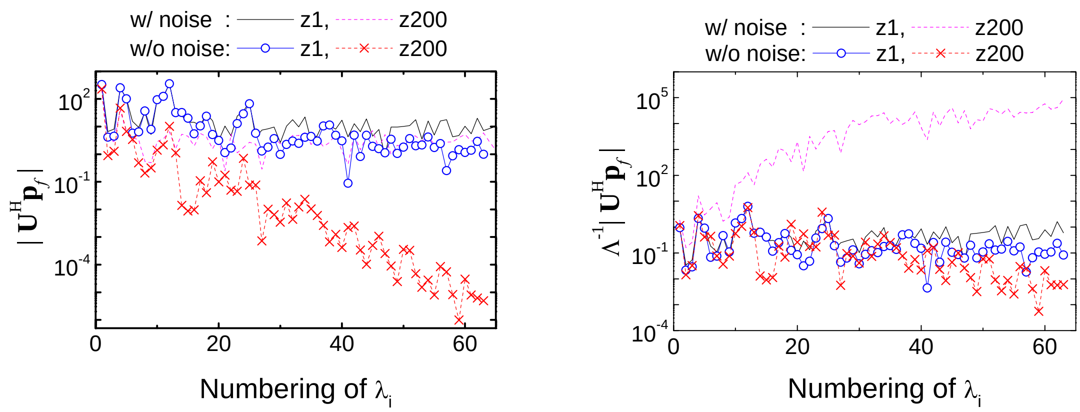

Fig. 7. A comparison of amplitudes of elements of $\mathbf{U}^H \mathbf{p}_f$ *and* $\Lambda^{-1}\mathbf{U}^H \mathbf{p}_f$ *vectors appearing in the inverse process.*

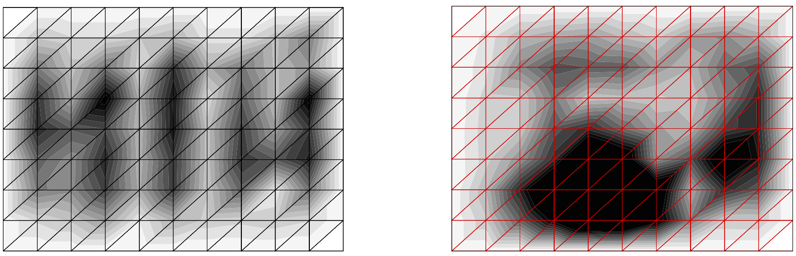

Fig. 8. Reconstructed velocity amplitude on the source surface before regularization: (a) z=1 mm, (b) z=200 mm.

incorporating bounding conditions during iteration steps. In this method, the choice of iteration number is most important due to the trade-off between the variance error arising from measurement error and the bias error resulting from regularization. A method for determining the optimal iteration number was suggested by Kim and Ih [33]. Most popularly used regularization techniques are Tikhonov regularization (TR) [34] and Landweber iteration method [35]. It is essential to find an optimal wave-vector filter shape by an optimal Tikhonov parameter or iteration number for proper regularization. Currently, there are various searching tools for an optimal parameter such as the mean-square error estimation using a noise variance σ^2 [23,33], sometimes referred as Morozov discrepancy principle [36], the generalized cross-validation technique [37], and the L-curve criterion [3], etc. To determine an optimal parameter, the golden section method or even genetic algorithms can be adopted [3,38,39]. A review of the regularization technique can be found in Ref. [40]. For example, a modified TR method uses the minimized Tikhonov functional Γ_2 as given by [34]

$$\Gamma_2 = \| \tilde{\boldsymbol{p}}_f - \mathbf{GQ} \|^2 + \alpha \| (\mathbf{I} - \boldsymbol{F}_1^{\alpha}) \boldsymbol{W}^H \mathbf{Q} \|^2 , \tag{9}$$

where α is a regularization parameter. Using this, one can obtain the solution of Eq. (7) as

$$\hat{\mathbf{Q}}_2^{\alpha} = \boldsymbol{W} diag\left(\cdots, \frac{\lambda_j (\alpha + \lambda_j^2)^2}{\alpha^3 + \lambda_j^2 (\alpha + \lambda_j^2)^2}, \cdots\right) \boldsymbol{U}^H \tilde{\boldsymbol{p}}_f = \boldsymbol{W} \boldsymbol{F}_2^{\alpha} \Lambda^{-1} \boldsymbol{U}^H . \tag{10}$$

Figure 9 shows the optimal wave vector filter shapes and filtered values of inverse singular values by using the iteration technique. In Fig. 10, we can observe that the inverted and filtered (regularized) transfer vectors for two measurement distances have decreasing trends with the increase of the order number of singular values. Figure 11 shows the final restored

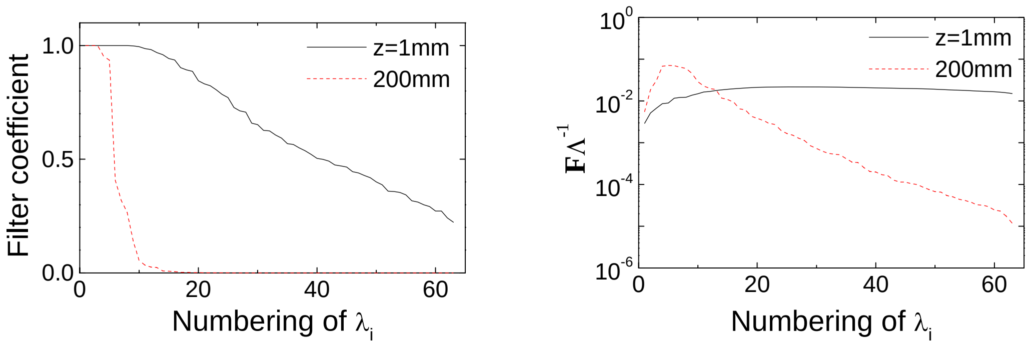

Fig. 9. (a) Coefficient of optimally designed wave vector filter, (b) amplitude of filtered and inverted singular values.

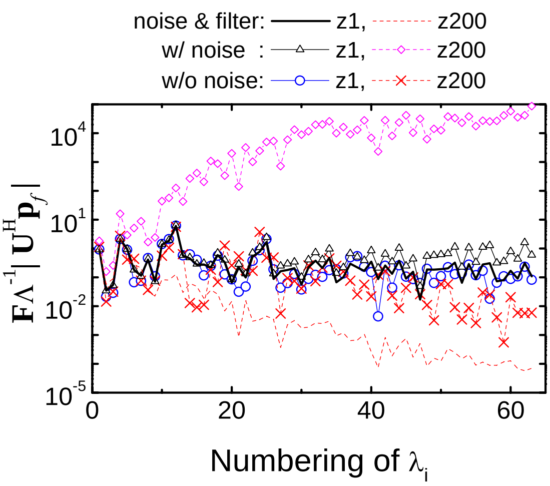

Fig. 10. A comparison of amplitudes of elements of $\mathbf{F}\Lambda^{-1}\mathbf{U}^H\mathbf{p}_f$ vectors (regularized).

image of the source velocity after regularization. One can find that the reconstructed source image from the nearfield data is very similar to the given velocity amplitude distribution; On the other hand, the source image recovered from the intermediate field data shows only the active contributing parts of the source to the field.

3. PRACTICAL APPLICATION EXAMPLES

Various sound sources have been tackled by the BEM-based NAH for the identification of vibro-acoustic sources. Examples include aircraft interior [41], refrigerator compressor [42], vacuum cleaner [16], internal combustion engine [16,43], vehicle interior [23], copying machines and printers [44], etc. Because the method permits the source identification of a complex shaped practical machinery, it is expected that the number of application cases will be increased very quickly.

Figure 12 shows the reconstructed surface intensity of an automotive engine as a demonstration example of the BEM-based NAH [16]. In the measurement of field pressure data, a 6-cylinder gasoline engine was driven by a dynamometer in a semi-anechoic chamber. The engine was modelled by 1047 nodes and 2148 linear triangular boundary elements. As input data, 1440 evenly spaced field pressure data were taken. The results at 150 Hz corresponds to the firing frequency (E3) at 3000 RPM. One can easily find the hot parts in sound radiation. Another application example can be seen: an irregular-shaped, three-dimensional machine, a canister-type vacuum cleaner. The vacuum cleaner was modelled by 170 nodes and 336 linear

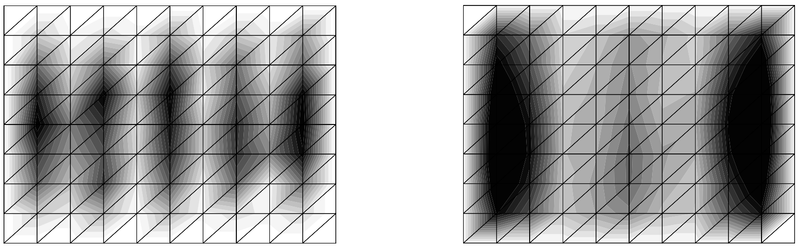

Fig. 11. Reconstructed velocity amplitude on the source surface after regularization: (a) z=1 mm, (b) z=200 mm.

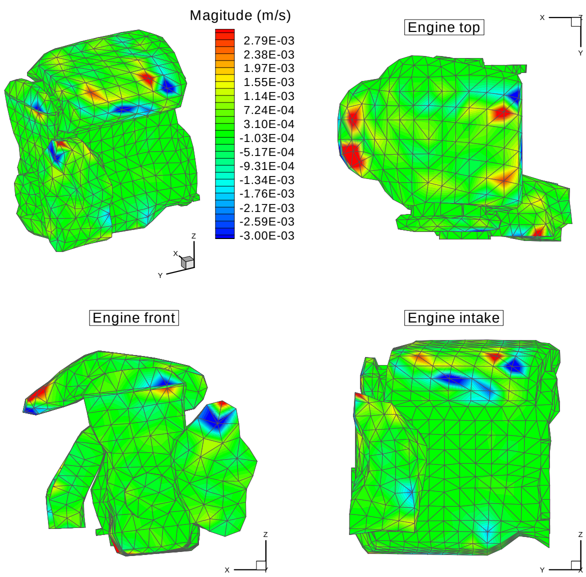

Fig. 12. Predicted magnitude of surface intensity of the engine at 150 Hz.

triangular boundary elements. Uniformly distributed 336 points were chosen as initial measurement positions. The parallelepiped hologram plane was separated from each nearest side of the vacuum cleaner by 60 mm. Target frequencies were 120 and 240 Hz, which were around the harmonic frequencies of the rotor installed inside the vacuum cleaner. Figure 13 shows the reconstructed surface velocity distribution [23].

Once the distributions of source parameters, *viz.*, sound pressure and particle velocity, are identified, one can employ the BEM model of the source again for the post-processing. Prediction of sound intensity (surface and field) in magnitude and flow vector, surface admittance, sound power, radiation efficiency, directivity, field pressure map, etc., are possible. A demonstration example for intensity vector flow and power is shown in Fig. 14 [45].

4. DISCUSSIONS ON THE FURTHER WORKS

Still, there are some problems for the BEM-based NAH technique. It is felt that we should conduct further studies to refine the technique for unrestricted and easy application to practical problems. The followings are part of features that we should consider about the enhanced command of the technique with precision or efficient practice.

4.1 Linear Independence Between Measurement Sensors

The linear independence of vibro-acoustic transfer matrix should be first assured by the proper allocation of measurement points on the hologram plane, irrespective of its shape. This can be accomplished by selecting the required number of points with the aid of an effective independence method [46]. The contribution of sensor position to the linear independence of a transfer matrix can be evaluated for a frequency range of interest and a point or set of points having the smallest value is discarded from the candidate sensor positions. Then, by repeating this process, one can define the measurement positions that are the least inter-dependent for a given number of measurement locations [16,23,47].

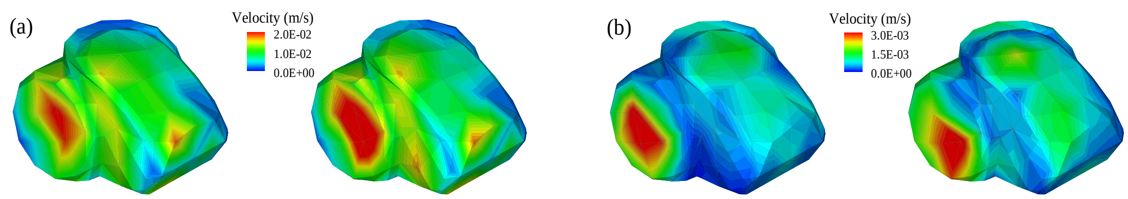

Fig. 13. Reconstructed normal surface velocities on the vacuum cleaner by the BEM-based NAH using 336 measured pressures (left column) and 336 regenerated pressures (60 internal fictitious sources for wave superposition) with 100 measured data (right column): (a) 120 Hz, (b) 240 Hz.

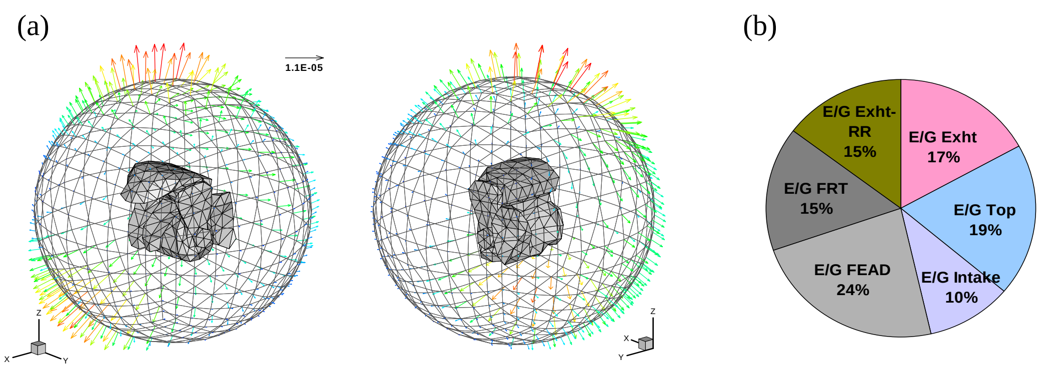

Fig. 14. An example of post processing of reconstructed source data of an engine in Fig. 12. (a) Sound intensity vector in the field, (b) pie chart showing the partial contribution rate to the total sound power.

4.2 Precision of Measurement and Reconstruction

In order to assure the measurement accuracy of the field data, sources of random and bias errors due to the mismatch of sensor positions and spacing, phase difference, small amplitude calibration, scattering from sensor fixtures, etc. should be suppressed and the influence of such measurement parameters should be monitored carefully. Error analysis for the planar spatial holography [48,49] can be partially applicable to the BEM-based NAH. Sensor proximity error to the source surface can be overcome when the non-singular or weakly singular BEM is employed in the modelling [50]. Errors associated with boundary element modelling should be taken into account [51] as well as the truncation error. If the information on a part of the source is known *a priori*, as is often the actual case, resolution enhancement of the restored result may be possible [52]. The effect of varying distance of the hologram plane to the source surface should be analysed and a compensation method or error analysis should be given. Most importantly, development of a new regularization technique should have a break though. Finally, one should remind that the time and spectral characteristics and magnitude of background noise are very much influential to the final reconstruction result [53]. All those aspects should be studied further in a statistical sense to obtain a fine restored result.

4.3 Speedy or Convenient Measurement for Engineering Application

In the practical measurement of the source, especially for large-scaled sources or source with many ancillaries attached to the source surface or sources with inaccessible part, partial measurement of the field data is inevitable. By an analogous implementation to the BEM-based NAH, data extrapolation technique [54] or so-called patched holography technique in spatial holography [55-57] are promising in solving the problem although one should accept certain level of errors, which may be acceptable in engineering sense. Measurement efforts and cost are too much in using the BEM-based NAH. Methods to countermeasure the measurement effort and time should be devised seriously. It was found that the use of reflecting bodies in the field, thus reducing the number of sensors, is useful [58] and the employment of ESM technique [16] combined with the BEM-based NAH can give a chance to virtually reduce the number of sensors and measurements, although some degradation of accuracy should be accepted in engineering sense.

4.4 Further Application to Interesting Topical Area

There remain many challenging application targets for the NAH. Possible topics include: Source visualization of rotating machinery, sound transmission analysis and imaging of insulation materials, identification in transient or impulsive operating condition, characterization of electro-magnetic sound generation field separated from the structural excitation, correlated analysis of acoustic and structural wave fields, etc. Recently, imaging of flow noise sources is one of hot research targets. The structures of jet noise, mixing noise and impinging noise source mechanisms related to the flow would be very challenging topics. Double stage inverse problem starting from the field data via the surface vibro-acoustic parameters to the internal source parameters would be a final target for the source identification [59], that would very helpful to prepare countermeasure plans of complicated noisy machinery. To conduct all these research topics, it is thought that new measurement and analysis techniques are required along with the development of new instrumentation techniques. For example, use of sound intensity data in the hologram plane would open a new window to the NAH technique [60]. Most important thing is that, needless to say, efficient and concrete countermeasure plans should be established after the reconstruction result of the source image is obtained.

5. CONCLUSIONS

The nearfield acoustical holography based on the inverse BEM was briefly reviewed notwithstanding the fact that the author might have a limited information on the recent progress in this area. This method enables the precise estimation of the distribution of acoustical parameters on the source surface, i.e., surface pressure and normal velocity on a vibrating object. From this inverse identification process, the radiation characteristics of the irregular source can be easily predicted. Sound radiation from a top plate of a parallelepiped box was adopted as a demonstration example to show the actual stage in implementing the NAH based on the inverse BEM. An automotive engine and a vacuum cleaner, having irregular shapes, were taken as practical application examples of the BEM-based NAH. On-going and future research topics were listed for the further refinement of the technique. Further development of new ideas may be borrowed from the theories for the ultrasonic imaging, tomography, digital image enhancement, and other fields using similar techniques, but under different disciplines. There is no doubt that one can extend the concept and method of BEM-based NAH to solve many challenging vibro-acoustic problems in practical machinery. A huge opportunity is open to the acousticians in this area by virtue of the recent brilliant development of computer and measuring instrument in data processing speed and memory size.

ACKNOWLEDGEMENTS

This work was partially supported by the BK21 Project. This paper contains many works collaborated with the former and present students of Acoustics Laboratory as parts of their Ph.D. theses at KAIST: B.-K. Kim at KIMM, S.-C. Kang at Doosan Infracore Co., I.-Y. Jeon at Samsung SDI Co., J.-H. Jeong at Hyundai Motor Co., S.-I. Kim at Samsung Electronics Co., J.-Y. Kim at Georgia Inst. Tech., H.-W. Jang, and A. Oey at KAIST.

REFERENCES

[1] H. W. Engl and C. W. Groetsch, *Inverse and Ill-Posed Problems*, Academic Press, Orlando, 1987.

[2] D. Colton and R. Kress, *Inverse Acoustic and Electromagnetic Scattering Theory*, Springer, Berlin, 1998, 2nd ed.

[3] P. C. Hansen, *Rank-Deficient and Discrete Ill-Posed Problems*, SIAM, Philadelphia, 1998.

[4] J.-G. Ih, "Inverse problems in the vibro-acoustics," Proc. of NOVEM 2005, St. Raphael, France, April 2005 (CD ROM).

[5] E. G. Williams and J. D. Maynard, "Holographic imaging without the wavelength resolution limit," Phys. Rev. Lett. **45**, 554-557 (1980).

[6] J. D. Maynard, E. G. Williams, and Y. Lee, "Nearfield acoustic holography: I. theory of generalized holography and the development of NAH," J. Acoust. Soc. Am. **78,** 1395-1413 (1985).

[7] J. D. Maynard, ''Acoustic holography for wideband, odd-shaped noise sources,'' Proc. Inter-noise 88, Avignon, France, September 1988, Vol. I, pp. 223–231.

[8] J. Hald, "STSF–a unique technique for scan-based near-field acoustic holography without restrictions on coherence," B&K Tech. Rev., No.1 (1989).

[9] K. Gardner and R. J. Bernhard, "A noise source identification technique using an inverse

Helmholtz integral equation method," Trans. ASME, J. Vib. Acoust. Stress Reliab. Des. **110**, 84-90 (1988).

[10] W. A. Veronesi and J. D. Maynard, "Digital holographic reconstruction of source with arbitrarily shaped surfaces," J. Acoust. Soc. Am. **85**, 588-598 (1989).

[11] G.-T. Kim and B.-H. Lee, ''3-D sound source reconstruction and field reprediction using the helmholtz integral equation,'' J. Sound Vib. **136**, 245-261 (1990).

[12] W. Williams, N. G. Parke, D. A. Moran, and C. H. Sherman, "Acoustic radiation from a finite cylinder," J. Acoust. Soc. Am. **36**, 2316-2322 (1964).

[13] Y-C. Chao, "An implicit least-square method for the inverse problem of acoustic radiation," J. Acoust. Soc. Am. **81**, 1288-1292 (1987).

[14] G. H. Koopmann, L. Song, and J. B. Fahnline, "A method for computing acoustic fields based on the principle of wave superposition," J. Acoust. Soc. Am. **86**, 2433-2438 (1989).

[15] J. B. Fahnline and G. H. Koopmann, "A numerical solution for the general radiation problem based on the combined methods of superposition and singular-value decomposition," J. Acoust. Soc. Am. **90**, 2808-2819 (1991).

[16] I.-Y. Jeon and J.-G. Ih, "On the holographic reconstruction of vibro-acoustic fields using equivalent sources and inverse boundary element method," J. Acoust. Soc. Am. **118**, 3473-3482 (2005).

[17] Z. Wang and S. F. Wu, "Helmholtz equation-least-squares method for reconstructing the acoustic pressure field," J. Acoust. Soc. Am. **102**, 2020-2032 (1997).

[18] S. F. Wu and X. Zhao, "Combined Helmholtz equation least-squares method for reconstructing acoustic radiation from arbitrary shaped objects," J. Acoust. Soc. Am. **112**, 179-188 (2002).

[19] S. Dumbacher and D. Brown, "Practical consideration of the IFRF method technique as applied to noise path analysis and acoustic imaging," Proc. of IMAC, Orlando, USA, 1997, 1677-1685.

[20] B.-H. Kim, B.-H. Park, I.-Y. Jeon, and J.-G. Ih, "Noise source ranking in automotive vehicle using the inverse FRF method," Proc. of Inter-Noise 2003, Seogwipo, Korea, August 2003 (CD-ROM).

[21] E. G. Williams, *Fourier Acoustics*, Academic Press, London, 1999, Chaps. 3,5,7,8.

[22] M. R. Bai, "Application of BEM (boundary element method)-based acoustic holography to radiation analysis of sound sources with arbitrarily shaped geometries," J. Acoust. Soc. Am. **92**, 533-549 (1992).

[23] B.-K. Kim and J.-G. Ih, "On the reconstruction of the vibro-acoustic field over the surface enclosing an interior space using the boundary element method," J. Acoust. Soc. Am. **100**, 3003-3016 (1996).

[24] Z. Zhang, N. Vlahopoulos, S. T. Raveendra, T. Allen, and K. Y. Zhang, ''A computational acoustic field reconstruction process based on an indirect boundary element formulation,'' J. Acoust. Soc. Am. **108**, 2167–2178 (2000).

[25] N. Valdivia and E. G. Williams, "Krylov subspace iterative methods for boundary element method based near-field acoustic holography," J. Acoust. Soc. Am. **117**, 711-724 (2005).

[26] D. M. Photiadis, "The relationship of singular value decomposition to wave-vector filtering in sound radiation problems," J. Acoust. Soc. Am. **88**, 1152-1159 (1990).

[27] J.-G. Ih and S.-C. Kang, "Meanings of SVD and wave-vector filtering in the near-field acoustical holography using the inverse BEM," J. Acoust. Soc. Am. **108**, pt.2, 2528 (2000).

[28] H. C. Andrews and B. R. Hunt, *Digital Image Restoration*, Prentice-Hall, Englewood Cliffs, New Jersey, 1977.

[29] H. Fleischer and V. Axelrad, "Restoring an acoustic source from pressure data using Wiener filtering," Acustica **60**, 172-175 (1986).

[30] H. Lee and D. P. Sullian, "Fundamental limitation of resolution enhancement by wave-field extrapolation," J. Acoust. Soc. Am. 84, 611-617 (1988).

[31] G. Demoment, "Image reconstruction and restoration: overview of common estimation structures and problems," IEEE Trans., Acoust. Speech Signal Process. **ASSP-37**, 2024-2036 (1989).

[32] J. Biemond, R. L. Lagendijk, and R. M. Mersereau, "Iterative methods for image deblurring," Proc. IEEE **78,** 856-883 (1990).

[33] B.-K. Kim and J.-G. Ih, "Design of an optimal wave-vector filter for enhancing the resolution of reconstructed source field by near-field acoustical holography (NAH)," J. Acoust. Soc. Am. **107**, 3289-3297 (2000).

[34] A. N. Tikhonov and V. Y. Arsenin, *Solutions of Ill-posed Problems*, Halsted Press, New York, 1977.

[35] A. Kirsch, *An Introduction to the Mathematical Theory of Inverse Problems*, Springer-Verlag, New York, 1996.

[36] E. G. Williams, "Regularization methods for near-field acoustical holography," J. Acoust. Soc. Am. **110**, 1976–1988 (2001).

[37] P. A. Nelson and S. H. Yoon, "Estimation of acoustic source strength by inverse methods: Part I, conditioning of the inverse problem," J. Sound Vib. **233**, 643–668 (2000).

[38] M.S. Bazaraa, H. D. Sheriali, and C. M. Shetty, *Nonlinear Programming: Theory and Algorithms*, John Wiley & Sons, New York, 1993.

[39] Z. Michalewicz, *Genetic Algorithms+Data Structures=Evolution Programs*, Springer-Verlag, New York, 1996.

[40] E. G. Williams, "Regularization methods for near-field acoustical holography," J. Acoust. Soc. Am. **110**, 1976-1988 (2001).

[41] E. G. Williams, B. H. Houston, P. C. Herdic, S. T. Raveendra, and B. Gardner, "Interior near-field acoustical holography in flight," J. Acoust. Soc. Am. **108**, 1451-1463 (2000).

[42] J.-G. Ih, S.-C. Kang, S.-J. Kim, and K.-S. Kang, ''Reconstruction of the vibro-acoustic field on the surface of the refrigerator compressor by using the BEM-based acoustic holography,'' Proc. of Int. Compressor Eng. Conference, Purdue, USA, 1998, 525–529.

[43] A. F. Seybert, "Forward and inverse numerical acoustics for NVH applications," Proc. of Int. Cong. Sound and Vib. (ICSV 9), Orlando, USA, July 2002 (CD ROM).

[44] Y. Sasaki, A. Mori, and A. Takanashi, "Noise source identification using I-BEM method," Proc. of Int. Congress on Acoust. (ICA2004), Kyoto, Japan, 2004 (CD ROM).

[45] J.-G. Ih, I.-Y. Jeon, and S.-I. Kim, "Holographic reconstruction of the vibro-acoustic field of an engine using the inverse BEM and equivalent sources," Proc. of Int. Cong. Sound and Vib. (ICSV 13), Vienna, Austria, July 2006 (CD ROM).

[46] D. C. Kammer, "Effect of modal error on sensor placement for on-orbit modal identification of large space structures," J. Guidance, Control, and Dynamics **15**, 334-341 (1992).

[47] M. R. La Grange, B. T. Berhaar, and N. B. Roozen, "Efficient BEM based acoustic imaging using the EfI method," Proc. of Int. Congress on Acoust. (ICA2004), Kyoto, Japan, 2004 (CD ROM).

[48] K.-U. Nam and Y.-H. Kim, "Errors due to sensor and position mismatch in planar acoustic holography," J. Acoust. Soc. Am. **106**, 1655-1665 (1999).

[49] K. Seijyou and S. Yoshikawa, "Reduction methods of the reconstruction error for large-scale implementation of near-field acoustical holography," J. Acoust. Soc. Am. **110**, 2007-2023 (2001).

[50] S.-C. Kang and J.-G. Ih, "Use of nonsingular boundary integral formulation for reducing errors due to near field measurements in the BEM-based NAH," J. Acoust. Soc. Am. **109**, 1320-1328 (2001).

[51] S. Marburg, "Six boundary elements per wavelength: Is that enough?" J. Comput. Acoust. **10,** 25-51 (2002).

[52] S.-C. Kang and J.-G. Ih, "The use of partially measured source data in near-field acoustical

holography based on the BEM," J. Acoust. Soc. Am. **107**, 2472-2479 (2000).

[53] M. Lee and J. S. Bolton, "Scan-based near-field acoustical holography and partial field decomposition in the presence of noise and source level variation," J. Acoust. Soc. Am. **107**, 382-393 (2006).

[54] K. Seijyou and S. Yoshikawa, "Reduction methods of the reconstruction error for large-scale implementation of near-field acoustical holography," J. Acoust. Soc. Am. **110**, 2007-2023 (2001).

[55] J. Hald, "Patch near-field acoustical holography using a new statistically optimal method," Proc. of Inter-Noise 2003, Seogwipo, Korea, August 2003 (CD ROM).

[56] E. G. Williams, B. H. Houston, and P. C. Herdic, "Fast Fourier transform and singular value decomposition formulations for patch nearfield acoustical holography," J. Acoust. Soc. Am. **114**, 1322–1333 (2003).

[57] M. Lee and J. S. Bolton, "Patch near-field acoustical holography in cylindrical geometry," J. Acoust. Soc. Am. **118**, 3721-3732 (2005).

[58] S.-I. Kim, J.-G. Ih, and J.-H. Jeong, "Use of rigid reflectors for the virtual increase of field data in the near-field acoustical holography," To appear in J. Comp. Acoust. (2007).

[59] R. H. Lyon, *Machinery Noise and Diagnostics*, Butterworths, Stoneham, 1987, Chaps. 4,7,8.

[60] F. Jacobsen and Y. Liu, "Near field acoustic holography with particle velocity transducers," J. Acoust. Soc. Am. **118**, 3139-3144 (2005).